Supplemental Material for Splashing of large helium nanodroplets upon surface collisions

Paul Martini[1,2] +, Simon Albertini[1,3] +, Felix Laimer[1], Miriam Meyer[1], Michael Gatchell[1,2], Olof Echt[1,4], Fabio Zappa[1,5] *, and Paul Scheier[1]

[1] Institut für Ionenphysik und Angewandte Physik, Universität Innsbruck, A-6020 Innsbruck, Austria

[2] Department of Physics, Stockholm University, 106 91 Stockholm, Sweden

[3] Management Center Innsbruck, Department Biotechnology & Food Engineering, A-6020, Austria

[4] Department of Physics, University of New Hampshire, Durham NH 03824, USA

[5] Departamento de Física, Universidade Federal de Juiz de Fora, MG, Brazil

[+] These authors contributed equally

* Correspondence should be addressed to Fabio.Zappa@uibk.ac.at

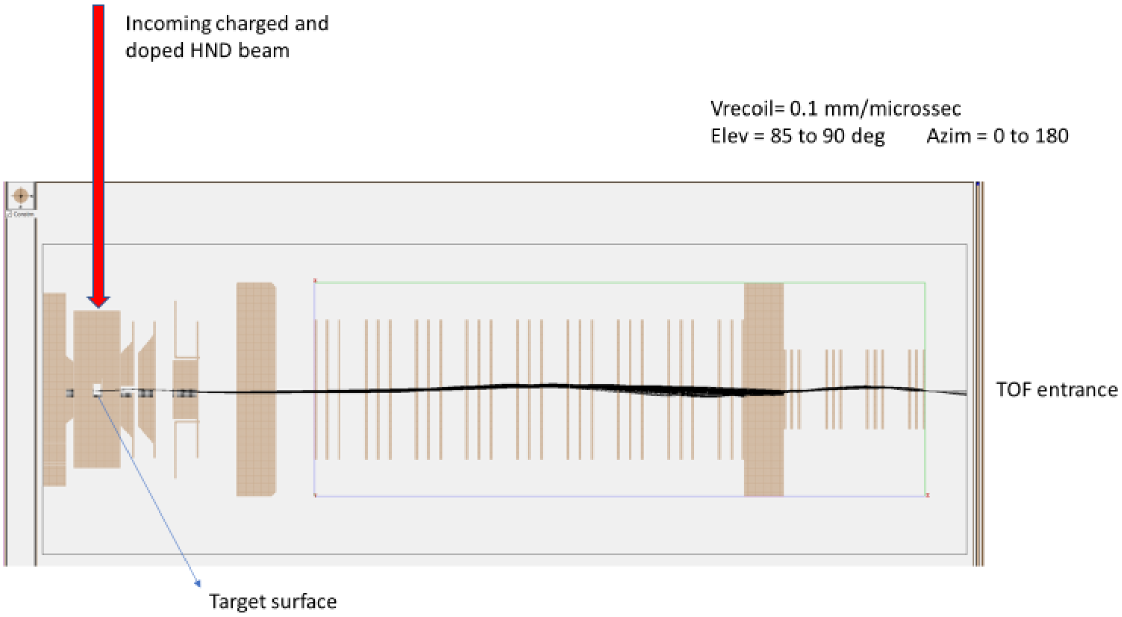

Figure S1 Simulation of the ion extraction for typical electrode settings, performed with the software SIMION. In this simulation singly-charged ions with a mass of 800 amu are assumed to originate from the target surface and have 100 m/s velocity pointing upwards. The extraction efficiency is found to be very sensitive to the initial kinetic energy and direction of the ions.

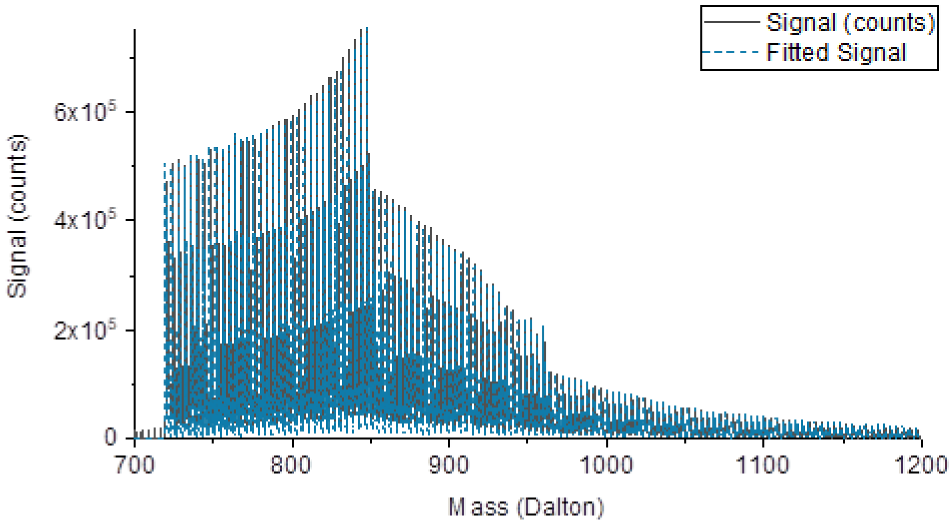

Figure S2. Grey line: Measured ion signal for the helium tagged C_{60} cations in the range between 700 Da and 1200 Da for the setup where the low mass ions were extracted from the HNDs after the collision with a stainless-steel surface (setup shown in Fig. 2b in the main text). The blue dashed line is the fitted curve of the signal performed with IsotopeFit [36].

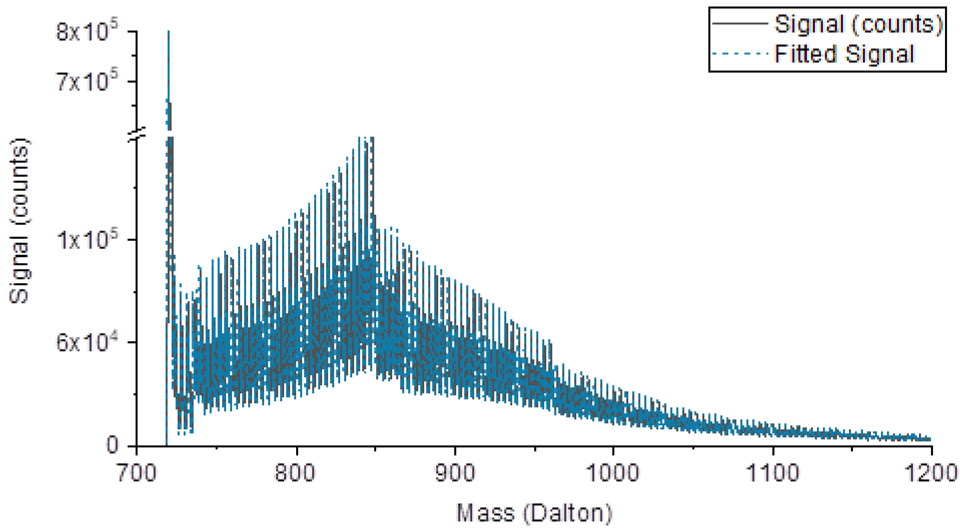

Figure S3. Grey line: Measured ion signal for the helium tagged C_{60} anions in the range between 700 Da and 1200 Da for the setup where the low mass ions were extracted from the HNDs after the collision with a stainless-steel surface (setup shown in Fig. 2b in the main text). The blue dashed line is the fitted curve of the signal performed with IsotopeFit [36].

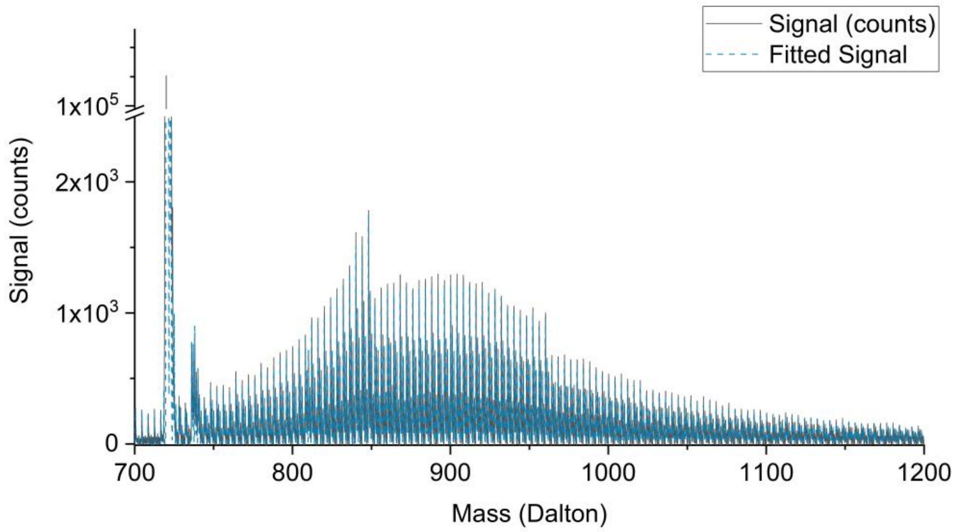

Figure S4. Grey line: Section of a mass spectrum showing helium tagged C_{60} cations in the range between 700 Da and 1200 Da for the setup where neutral HNDs doped with C_{60} were ionized with 70 eV electrons (setup shown in Fig. 2a in the main text). The blue dashed line is the fitted curve of the signal performed with IsotopeFit [36].

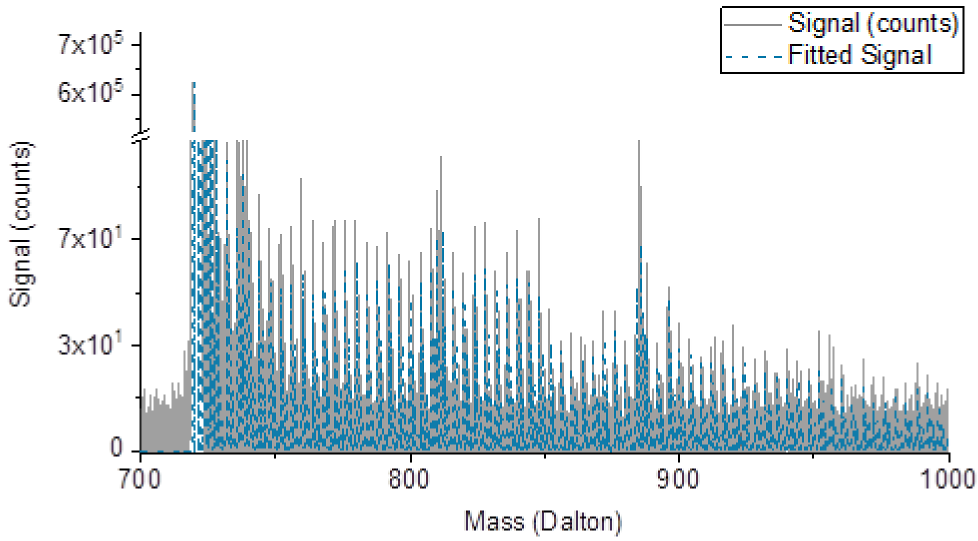

Figure S5. Grey line: Section of a mass spectrum showing helium tagged C_{60} anions in the range between 700 Da and 1000 Da for the setup where neutral HNDs doped with C_{60} are ionized with 22 eV electrons (setup shown in Fig. 2a in the main text). The blue dashed line is the fitted curve of the signal performed with IsotopeFit [36].

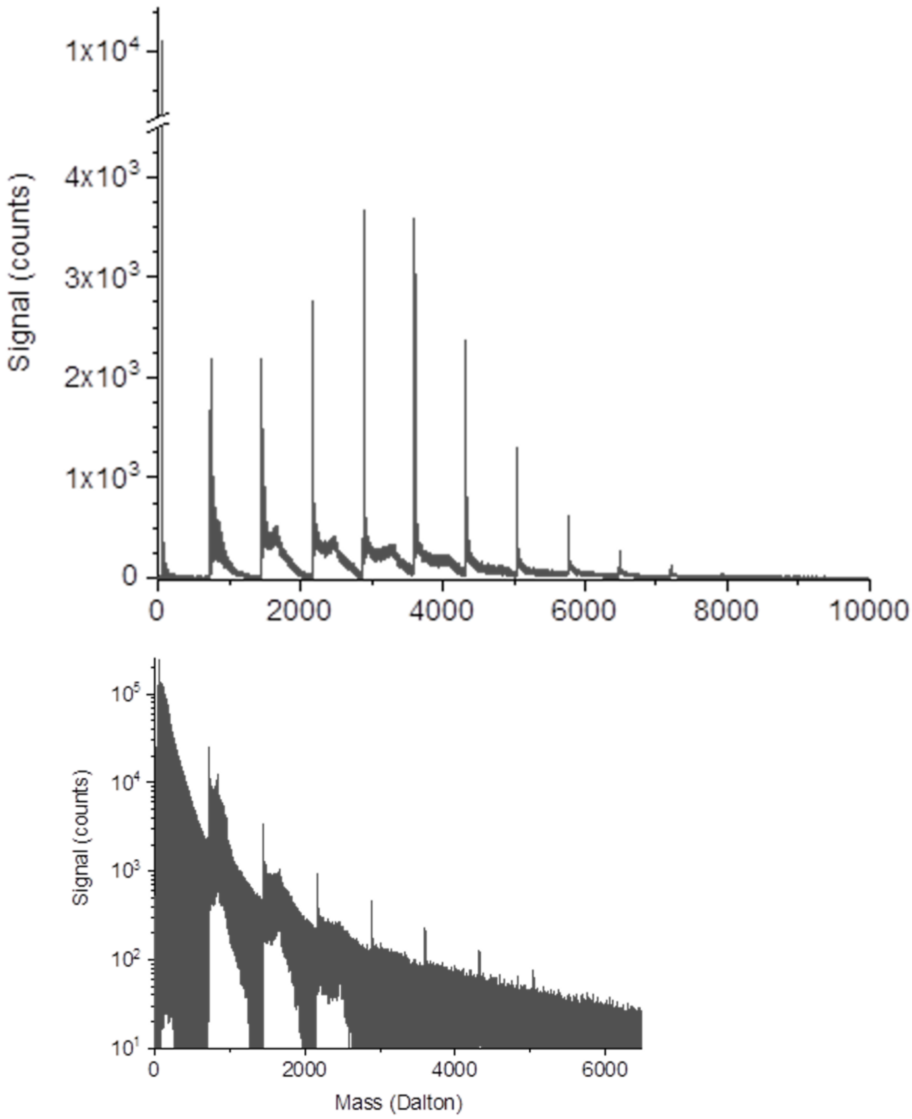

Figure S6 Mass spectra of anions and cations (top and bottom panels respectively) backscattered upon surface collisions of charged HNDs doped with C_{60}. The droplet formation and pickup conditions for both measurements are identical. In the case of anions, neutral HNDs were ionized by electron bombardment with a 27 eV and 345 μA electron beam, whereas cations were obtained by electron ionization with a 57 eV and 385 μA electron beam.

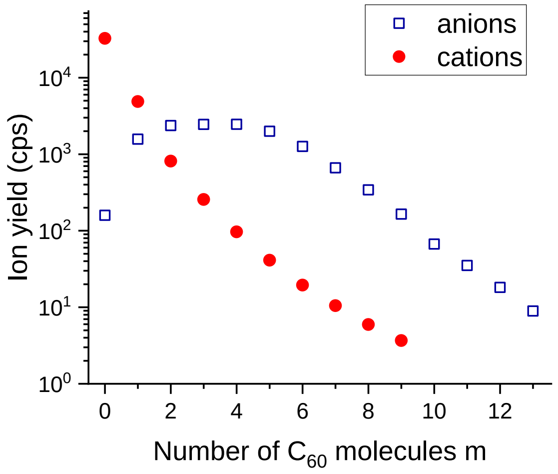

Figure S7. Abundance of $(C_{60})_m^{\pm}$ ions detected via surface collisions of charged HNDs doped with C_{60}. Each data point was obtained via summation of the contributions of differently tagged $He_n(C_{60})_m^{\pm}$ ions ($n \geq 0$). The error bars are smaller than the symbol size. The average droplet size for both polarities is roughly four million He atoms per droplet. Data points for m = 0 represent the sum of all pure helium cluster ions.

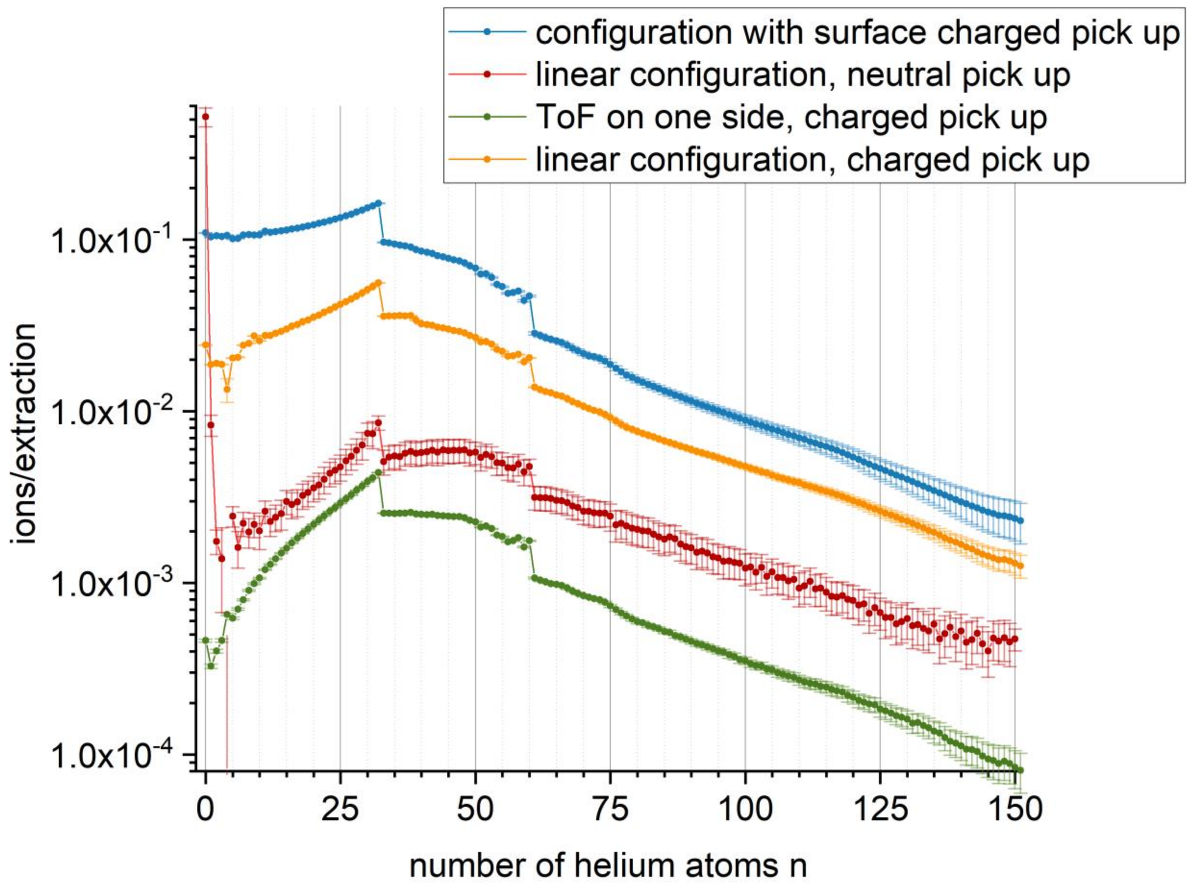

Figure S8. The ion signal per extraction pulse of the TOF as a function of the number of helium atoms n attached to singly charged fullerene cations for different configurations of the experimental setup. The red curve shows the signal obtained with the original setup (see Fig. 2b in the main text) with the pick up into neutral HNDs and the TOF mass spectrometer in the trajectory of the HNDs beam. The yellow curve shows the same experimental configuration but the ionization and the pick up sequence is reversed. For this case the repulsion of the charge centers inside the HNDs forces the ions towards the surface region of the HNDs, which makes the ejection of the ions more likely in the extraction region of the TOF. The green curve shows ions with pick up into charged HNDs but the TOF mass spectrometer was moved by 90 degree with respect to the flight path of the HNDs. The low ion yield indicates the inefficient extraction of the ions. The blue curve shows the ion yield of the surface setup (Fig. 2a in the main text).

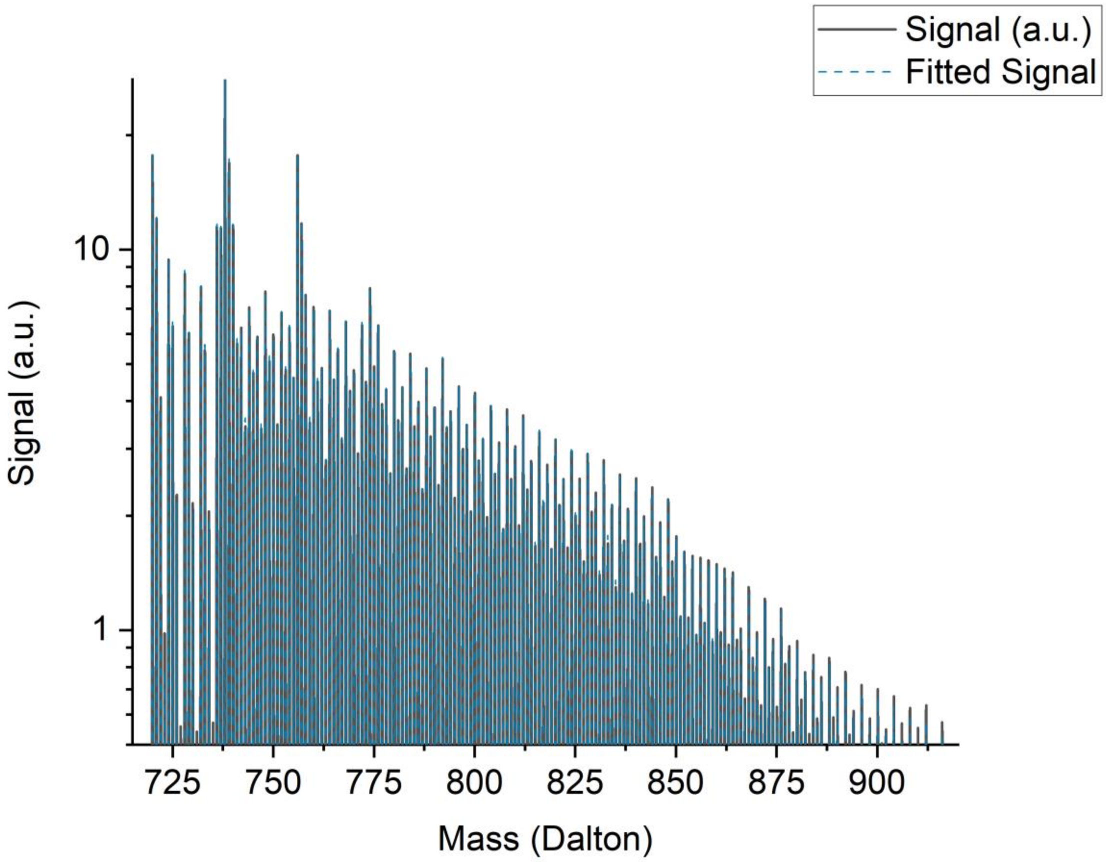

Figure S9. Section of a mass spectrum of He tagged C_{60} cations obtained with the experimental setup described in ref [35]., Positively charged HNDs were doped with C_{60} molecules and subsequently these He-tagged ions were extracted from the droplets by evaporation of the HNDs via multiple collisions with stagnant He gas at room temperature in a RF hexapole ion guide. The $C_{60}(H_2O)_mHe_n^+$ ions were most likely formed by pickup of water impurities (1ppm stated by the supplier) in the He collision gas. The mass difference between $C_{60}(H_2O)_{m+2}He_n$ and $C_{60}(H_2O)_mHe_{n+9}$ is only 0.0023 Dalton which requires a mass resolution m/Δm>321 000 to separate them.

For the investigation of the large Bi clusters formed in the HNDs and their splashing behavior two different grids were used. One was placed directly in the path of the HNDs beam (G1) and on the side

(G2) for the deposition of sideways scattered Bi clusters. For each TEM grid, three TEM images at three different positions were taken.

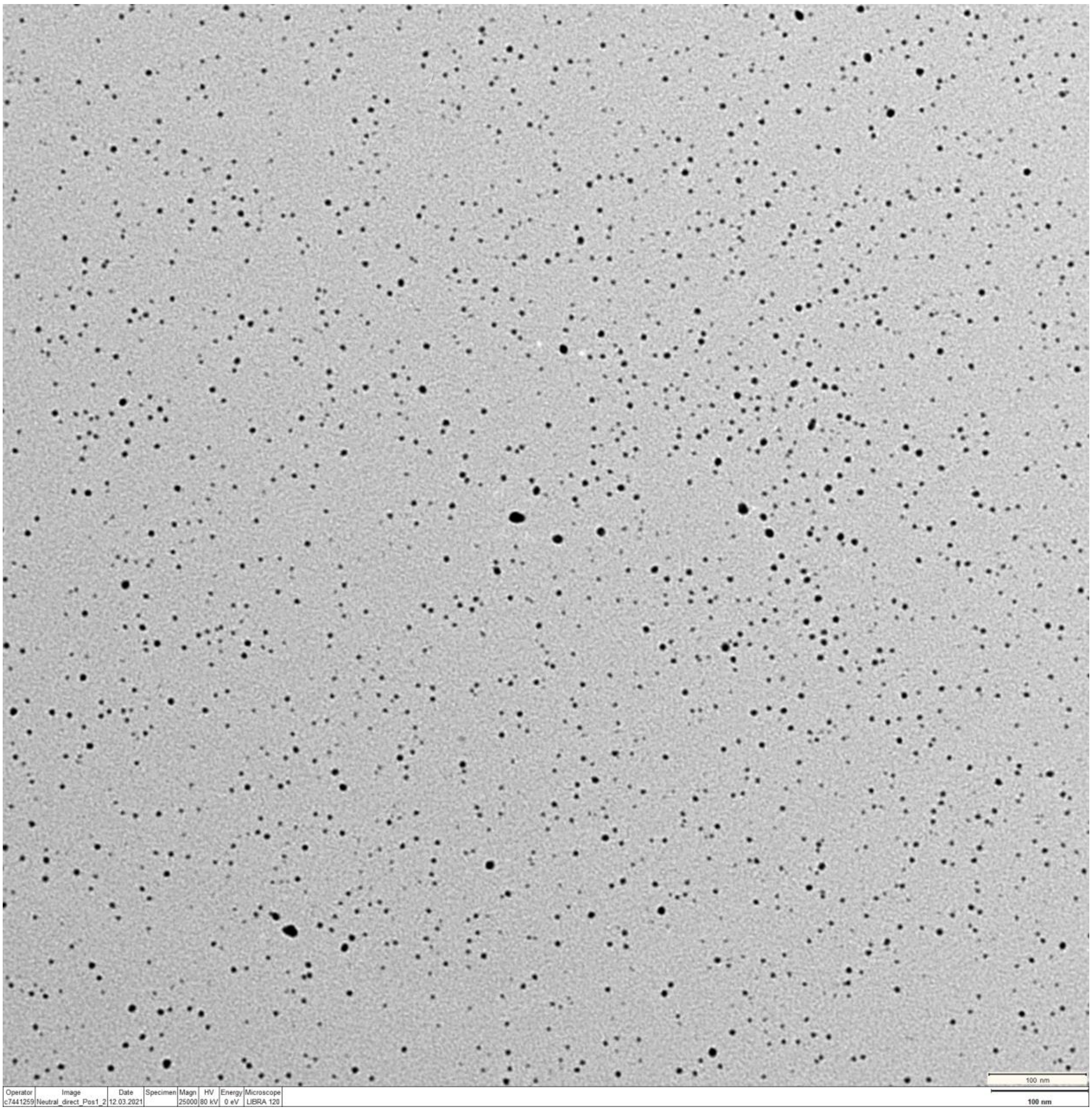

Figure S7 TEM image showing the deposited neutral Bi clusters formed in the HNDs. This TEM grid was placed in the path of the HNDs (0 deg, G1) position 1.

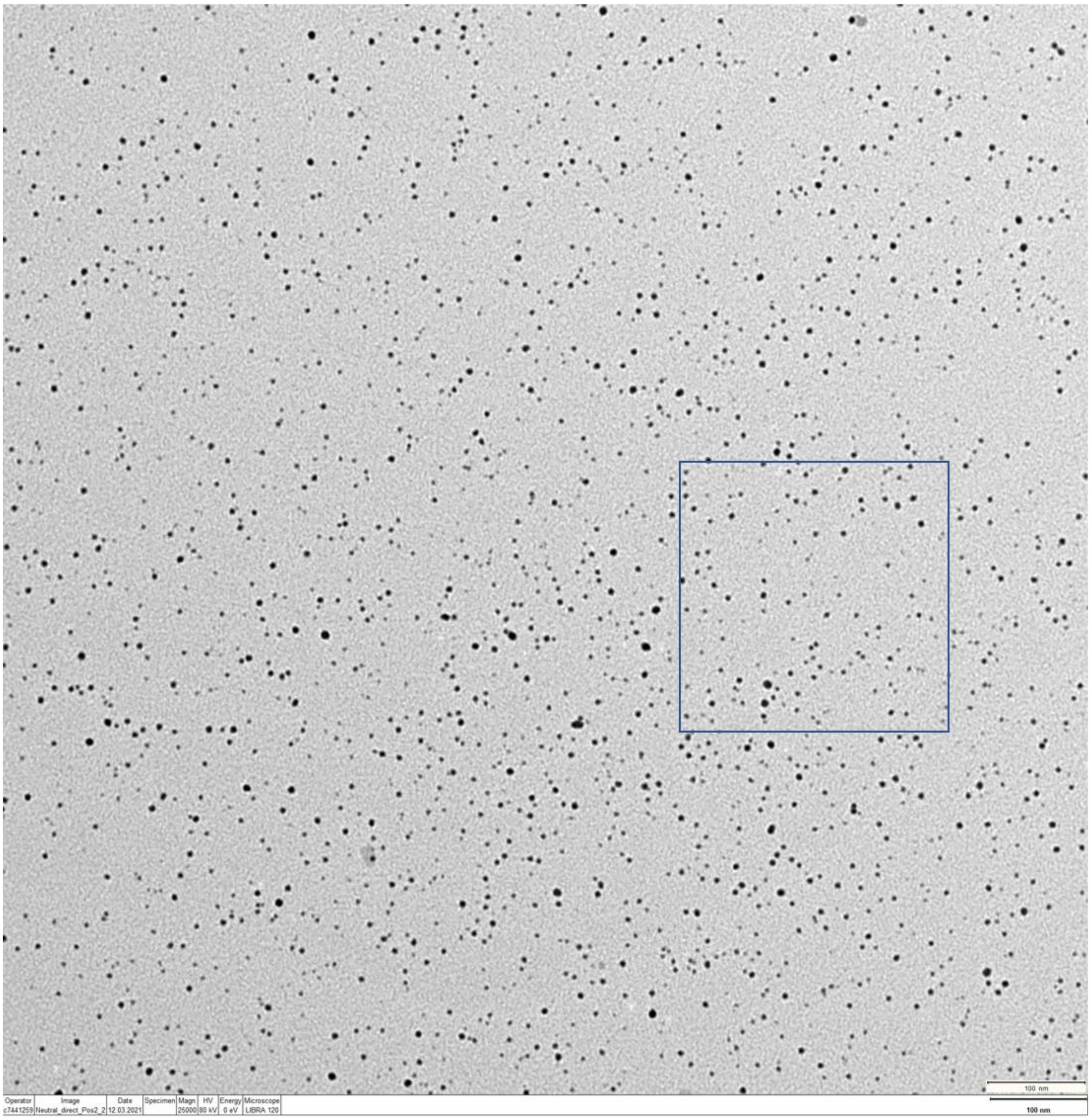

Figure S8 TEM image showing the deposited neutral Bi clusters formed in the HNDs. This TEM grid was placed in the path of the HNDs (0 deg, G1) position 2. The blue square shows the part of the image shown in Figure 1 of the main text.

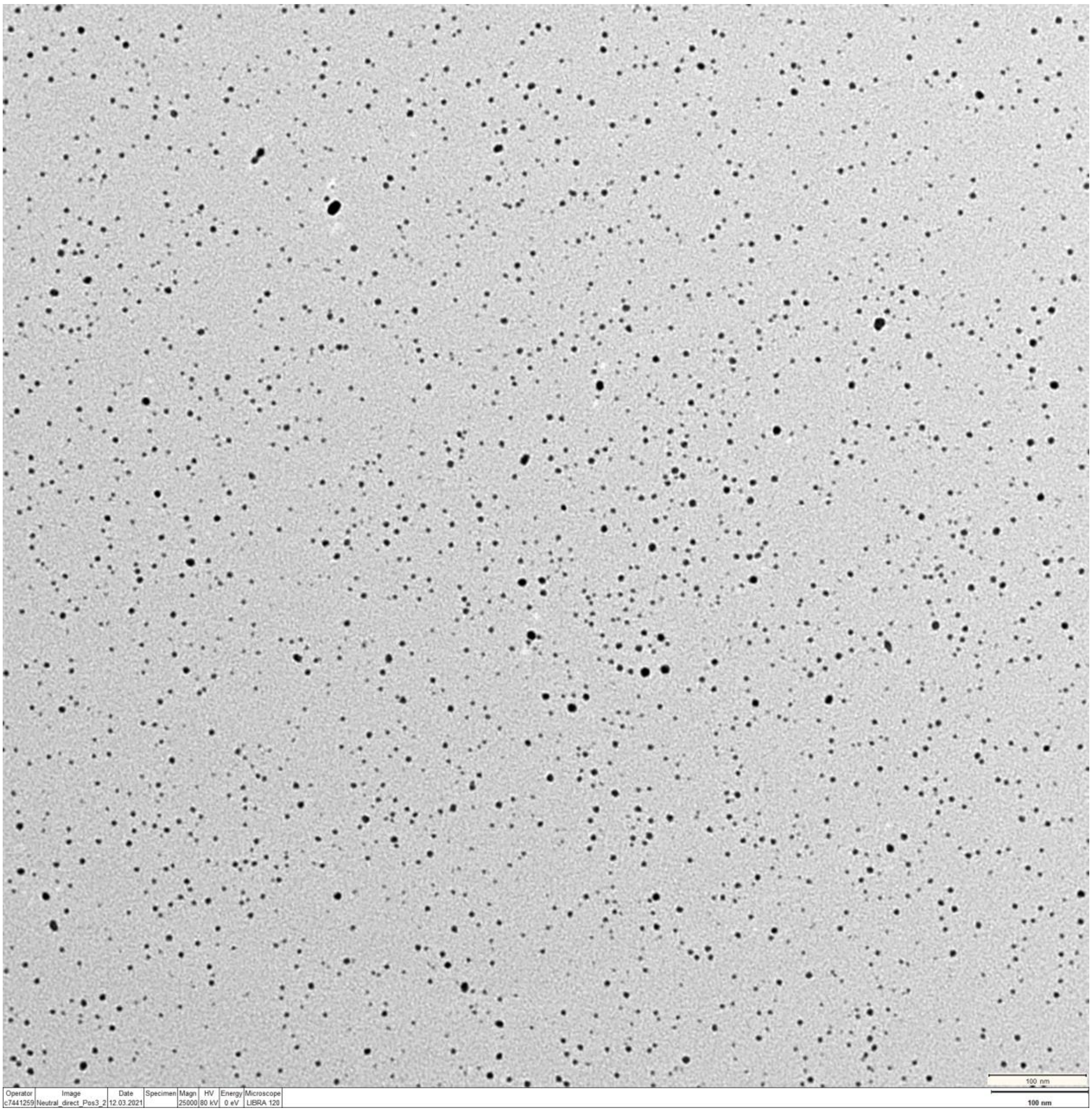

Figure S9 TEM image showing the deposited neutral Bi clusters formed in the HNDs. This TEM grid was placed in the path of the HNDs (0 deg, G1) position 3.

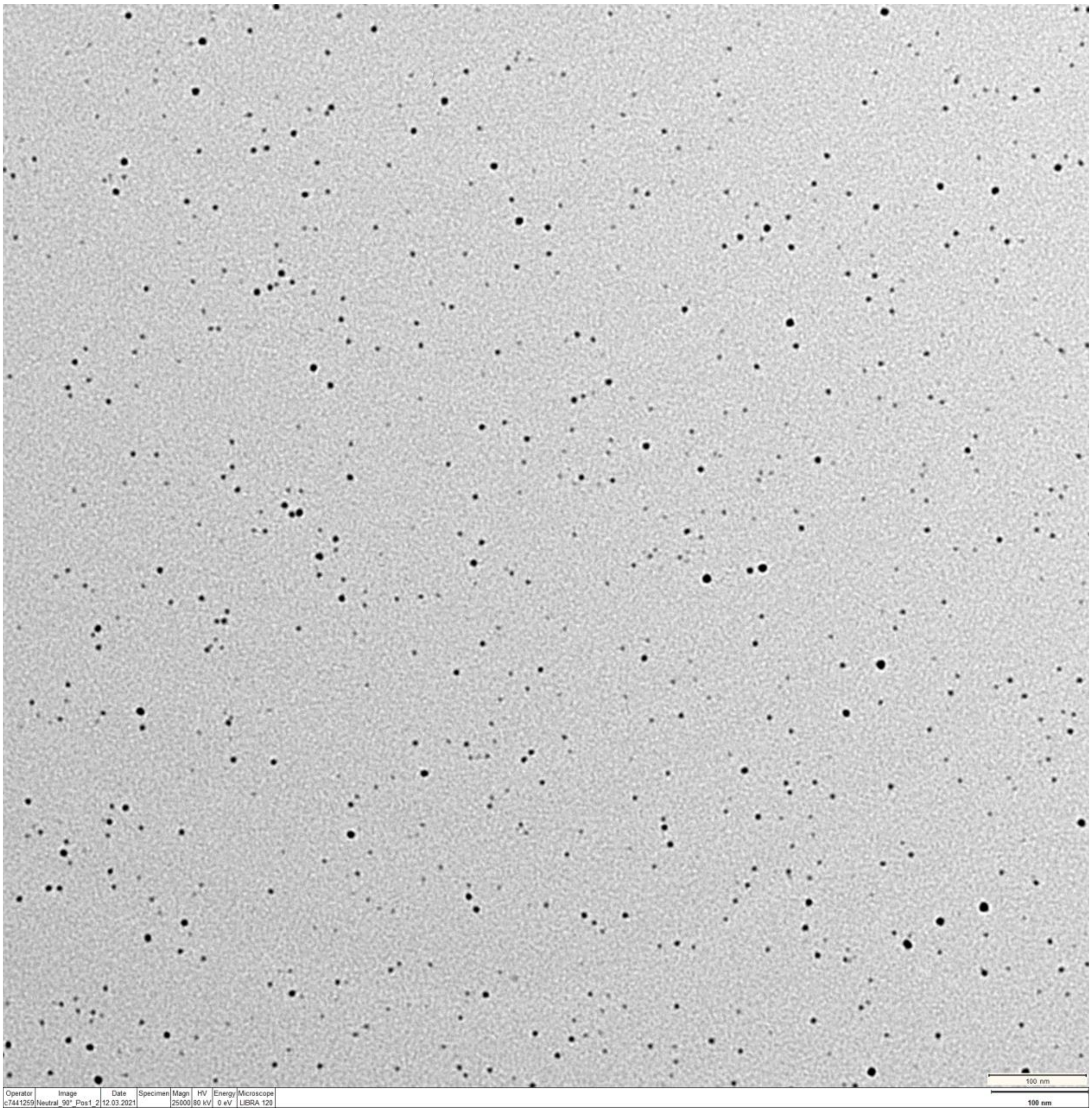

Figure S10 TEM image showing the deposited neutral Bi clusters after the splashing of the HNDs. This TEM grid was placed on the side (90 deg, G2) position 1.

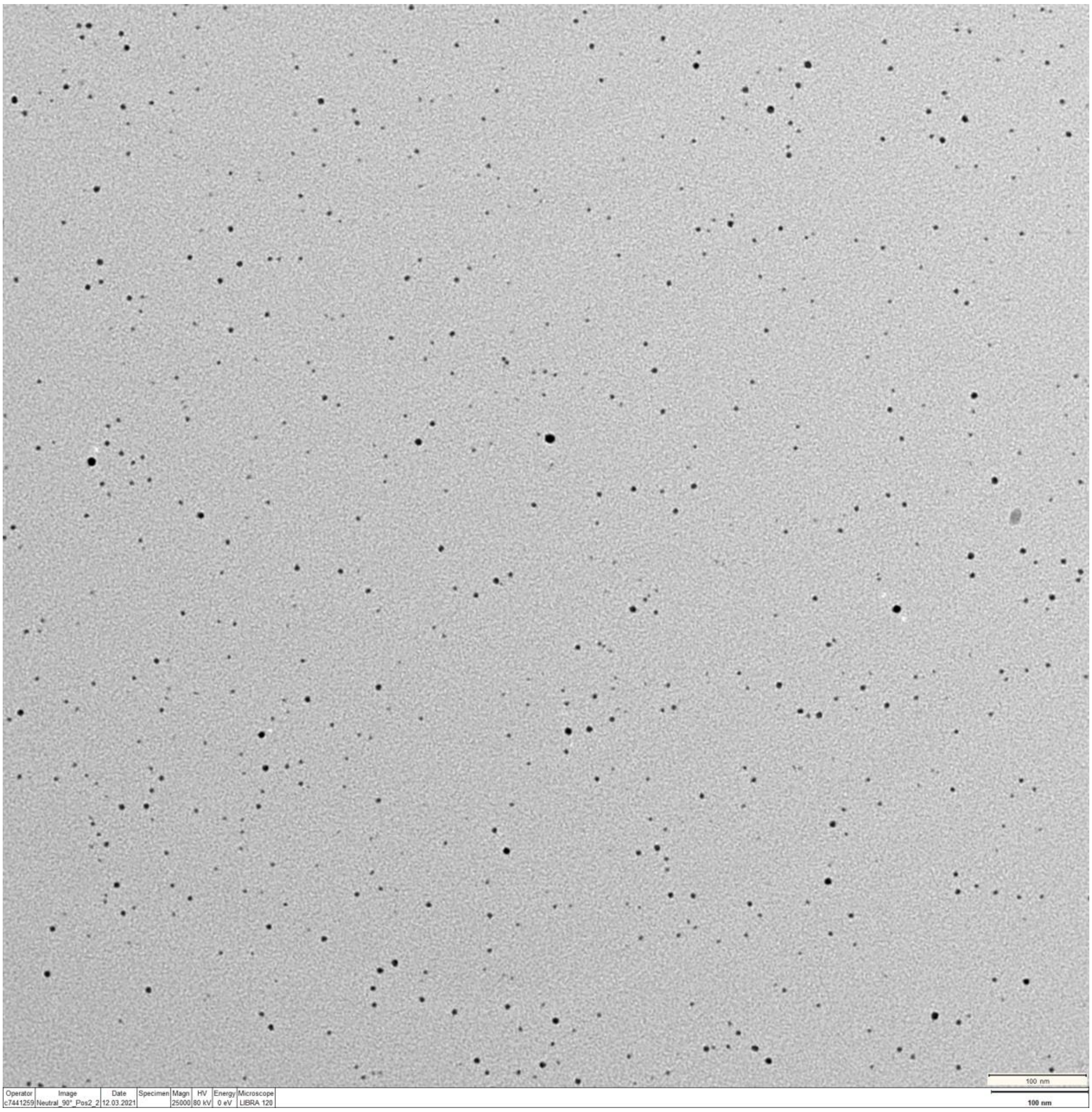

Figure S11 TEM image showing the deposited neutral Bi clusters after the splashing of the HNDs. This TEM grid was placed on the side (90 deg, G2) position 2.

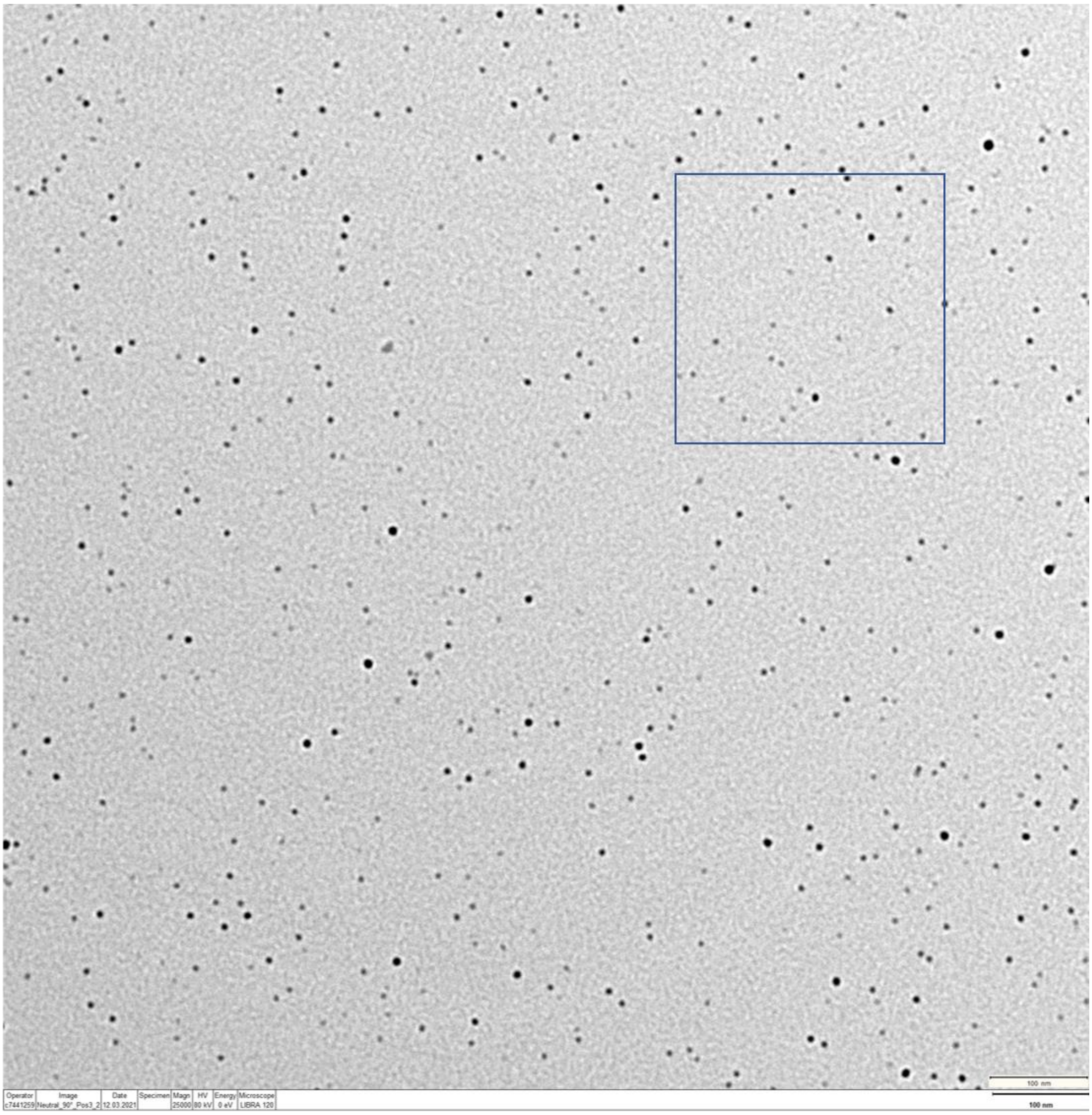

Figure S12 TEM image showing the deposited neutral Bi clusters after the splashing of the HNDs. This TEM grid was placed on the side (90 deg, G2) position 3. The blue square shows the part of the image presented in the main text.

For the analysis of the TEM images the three images showed above for the deposition of neutral Bi cluster for both, directly (G1) and on the side (G2) were analyzed with the program CellProfiler [30]. The results for the cluster size distribution of both cases as shown in the histograms in Figure S15 (G1) and S16 (G2). The resolution of the TEM allowed only a meaningful detection of clusters with a diameter >1.65nm. Possible clusters with a diameter small than 1.65nm were neglected because they were not clearly distinguishable from the background of the images.

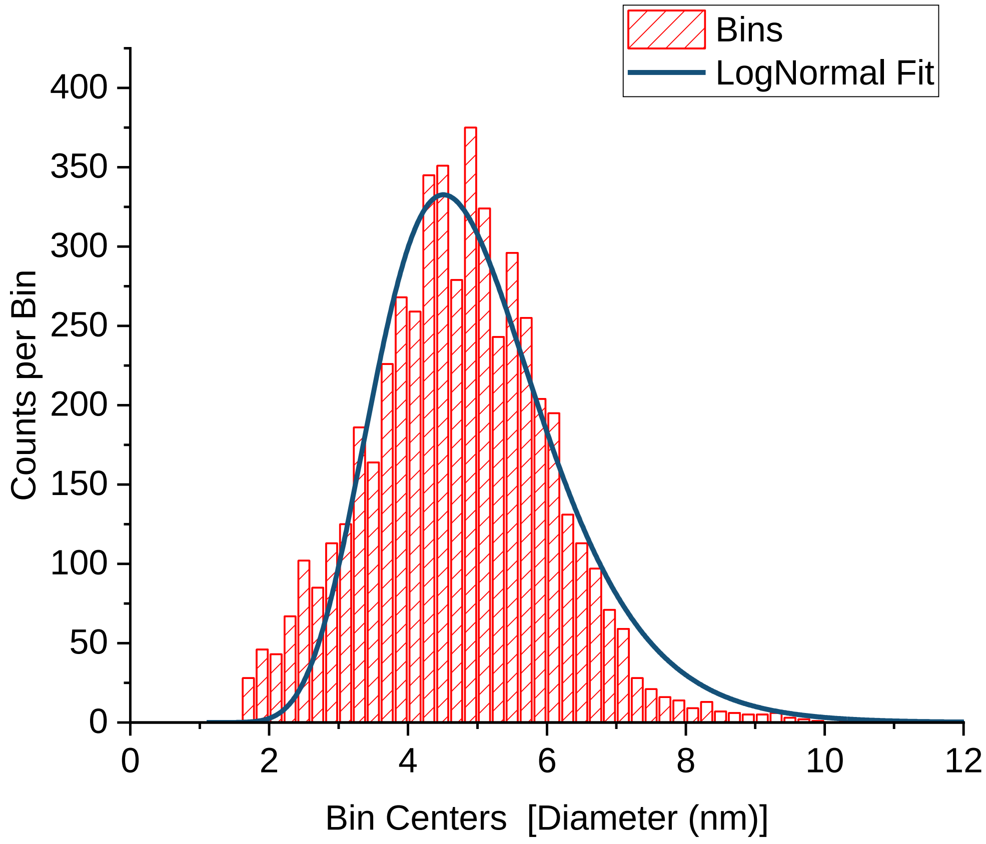

Figure S136 The size distribution of clusters shown in Fig. S10, S11 and S12 recognized by the program CellProfiler [30] as a function of the calculated diameter of the clusters. For this histogram a bin size of 0.2 nm was used. The obtained distribution for the direct (on TEM grid G1) deposition neutral Bi clusters is fitted here with a lognormal distribution shown in blue.

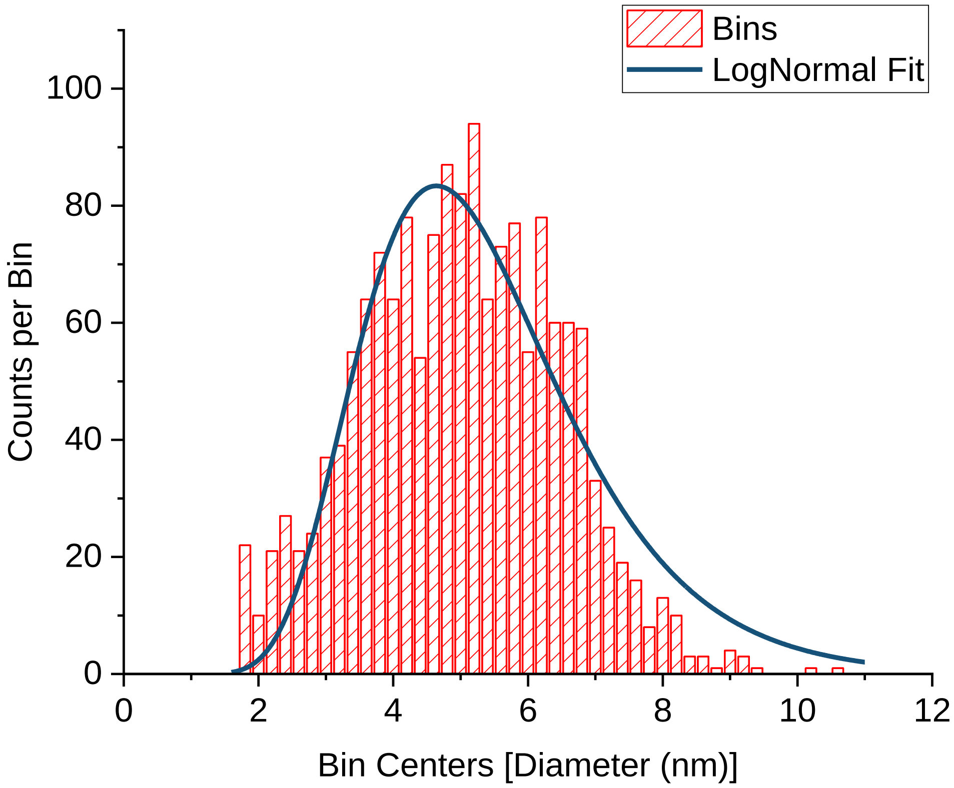

Figure S17 The size distribution of clusters shown in Fig. S13, S14 and S15 recognized by the program CellProfiler [30] as a function of the calculated diameter of the clusters. For this histogram a bin size of 0.2 nm was used. The obtained distribution for the direct (on TEM grid G1) deposition neutral Bi clusters is fitted here with a lognormal distribution shown in blue.

References

[30] M. R. Lamprecht, D. M. Sabatini, and A. E. Carpenter, Biotechniques 42, 71 (2007).
[35] L. Tiefenthaler, J. Ameixa, P. Martini, S. Albertini, L. Ballauf, M. Zankl, M. Goulart, F. Laimer, K. von Haeften, F. Zappa, and P. Scheier, Rev Sci Instrum 91, 033315 (2020).
[36] S. Ralser, J. Postler, M. Harnisch, A. M. Ellis, and P. Scheier, Int J Mass Spectrom 379, 194 (2015).